

Ginzburg–Landau equations with consistent Langevin terms for nonuniform wires

Jorge Berger

Physics Department, Ort Braude College,

P. O. Box 78, 21982 Karmiel, Israel and

*Department of Physics, Technion, 32000 Haifa, Israel**

Abstract

Many analyses based on the time-dependent Ginzburg–Landau model are not consistent with statistical mechanics, because thermal fluctuations are not taken correctly into account. We use the fluctuation-dissipation theorem in order to establish the appropriate size of the Langevin terms, and thus ensure the required consistency. Fluctuations of the electromagnetic potential are essential, even when we evaluate quantities that do not depend directly on it. Our method can be cast in gauge-invariant form. We perform numerous tests, and all the results are in agreement with statistical mechanics. We apply our method to evaluate paraconductivity of a superconducting wire. The Aslamazov–Larkin result is recovered as a limiting situation. Our method is numerically stable and the nonlinear term is easily included. We attempt a comparison between our numerical results and the available experimental data. We found no evidence for phase slips. We studied the behavior of a moderate constriction.

PACS numbers: 05.10.Gg, 74.40.+k, 05.40.-a, 02.70.Bf

*Electronic address: phr76jb@tx.technion.ac.il

I. INTRODUCTION

Almost a century ago Langevin [1] proposed a “complementary” stochastic force in order to enable the description of an individual Brownian particle in terms of Newton’s second law. This approach gave origin to the field of stochastic differential equations.

Among the many widely used stochastic differential equations, we will focus on the time-dependent Ginzburg–Landau equations (TDGL), which are used to describe a superconductor out of equilibrium [2]. The TDGL equations may be written in the form

$$\gamma\hbar\partial_t\psi = -[\alpha + \beta|\psi|^2 + |\alpha|\xi^2(i\nabla - 2\pi\mathbf{A}/\Phi_0)^2]\psi, \quad (1)$$

$$\sigma\partial_t\mathbf{A} = (2\hbar ce/m)\text{Re}[\psi^*(i\nabla - 2\pi\mathbf{A}/\Phi_0)\psi] - (c^2/4\pi)\nabla \times \nabla \times \mathbf{A}, \quad (2)$$

where ψ is the order parameter, \mathbf{A} the electromagnetic vector potential, t the time, ξ the coherence length, $\Phi_0 = hc/2e$ the quantum of magnetic flux, α , β and γ are material parameters, c is the speed of light, e the absolute value of the electron charge, m the mass of a Cooper pair and the asterisk denotes complex conjugation. β and γ are positive, whereas α is positive above the critical temperature and negative below it. The product $|\alpha|\xi^2 = \hbar^2/2m$ does not depend on the temperature. In these equations the gauge choice eliminates the scalar potential.

In order to cope with fluctuation problems, Schmid added a Langevin term to these equations [3]. Precisely, he added to the right-hand side of Eq. (1) a random function of position and time, $f(\mathbf{r}, t)$, such that

$$\langle f^*(\mathbf{r}, t)f(\mathbf{r}', t') \rangle = 2V\hbar\gamma k_B T \delta(\mathbf{r} - \mathbf{r}')\delta(t - t'), \quad (3)$$

where $\langle \dots \rangle$ denotes ensemble average, V is the volume of the sample, k_B is Boltzmann’s constant and T is the temperature. Since then the use of a Langevin term has become almost a standard practice in the numeric solution of the TDGL equations. Some miscellaneous examples are [4, 5, 6, 7].

We know from previous works [8, 9, 10] that a superconducting wire with nonuniform cross section may behave qualitatively differently than a uniform wire, especially near the transition temperature. We are therefore interested in a numeric scheme that can enable us to investigate nonuniform wires in the region in which thermal fluctuations are important.

The existing literature for integration of the TDGL equations by means of Euler-Maruyama iterations is not readily helpful, because the procedure for evaluating the size of the fluctuations of the order parameter in each computational site is not spelled out. In particular, we have not found any explanation that relates this size to the volumes of the computational cells. In addition, with rare exceptions [11, 12], only the fluctuation term in Eq. (3) is taken into account and fluctuations of the electromagnetic field are ignored. This approach is not self-consistent, even if we are only interested in the values of the order parameter.

In this article we build the equations for the evolution of a nonuniform superconducting wire, as appropriate for a finite difference numeric treatment. For this purpose we first discretize the the TDGL thermodynamic potential and then invoke the fluctuation-dissipation theorem [13] to evaluate the self-consistent Langevin terms.

II. OUR METHOD

A. The fluctuation-dissipation theorem

For our purposes, the theorem may be stated as follows. We consider a system with energy G that depends on several variables, one of which is x . Let the system be in thermal contact with a heat bath at temperature T and let x be a classical variable, i.e., a real function of time. Let x obey on the average the macroscopic equation

$$dx/dt = -\Gamma\partial G/\partial x . \quad (4)$$

Let τ be a macroscopically short period of time. Then the microscopic change of x , $x(t + \tau) - x(t)$, will be $-\Gamma\tau\partial G/\partial x$ on the average and its variance will be

$$\langle\eta^2\rangle = 2\Gamma k_B T \tau , \quad (5)$$

where $\eta = x(t + \tau) - x(t) + \Gamma\tau\partial G/\partial x$.

The physical idea behind this theorem is the same as in the original Langevin article, i.e., the same interactions of the variable x with the heat bath, that give origin to its microscopic fluctuations, are those that lead to its macroscopic evolution in Eq. (4).

Several assumptions are necessary for the validity of this theorem. One of them is that the distribution of the coordinates of the heat bath that interact with x remain described by the

canonical ensemble. There are also conditions on the size of τ ; it has to be macroscopically small, quantitatively expressed by $\tau \ll k_B T / \Gamma (\partial G / \partial x)^2$ and $\tau \ll 1 / \Gamma \partial^2 G / \partial x^2$. On the other hand, τ has to be microscopically large, explicitly, much larger than the autocorrelation time of the Langevin term and also large enough to allow for a classical treatment of x . From the numerical point of view, taking a value of τ that is too small may be a waste of resources but, in principle, should not affect the results. Indeed, if we take a time step τ/K rather than τ , the average and the variance of the change in x will decrease by the factor K , so that, if η has Gaussian distribution, after K steps the ensemble of results will be the same as if the time step were τ .

B. Ginzburg-Landau energy

In this model the energy of a superconducting wire can be written as

$$G = \int [\alpha |\psi|^2 + \beta |\psi|^4 / 2 + |\alpha| \xi^2 |(i \nabla - 2\pi \mathbf{A} / \Phi_0) \psi|^2 + IA / cw] dV, \quad (6)$$

where the integral is over the volume of the wire. Here I is the current that flows along the wire, w is its cross section, and the last term in the integrand takes into account the energy provided by the power source. We consider a wire with a cross section that is much smaller than the square of the magnetic penetration depth, so that the induced magnetic field can be neglected. In this situation we are also allowed to take the electromagnetic potential \mathbf{A} in the direction of the wire. Likewise, we will assume that the width of the wire is small compared to the coherence length and varies slowly with the arc length; for the superconducting-insulator boundary condition these assumptions imply that ∇ may be replaced with the derivative with respect to the arc length.

Let us now discretize this energy. We denote the length of the wire by L and divide it into N segments of length L/N . Each segment has to be sufficiently short, so that the order parameter, the electromagnetic potential and the cross section may be considered to remain uniform along them, and we denote them by ψ_k , A_k and w_k for the k^{th} segment. Defining the grid-dependent dimensionless variables $\tilde{\xi} = N\xi/L$ and $\tilde{A} = 2\pi LA/N\Phi_0$, we may write

$$G = \frac{L}{N} \sum w_k \left\{ \alpha |\psi_k|^2 + \beta |\psi_k|^4 / 2 + \frac{|\alpha|}{2} \tilde{\xi}^2 \left[|(1 + i\tilde{A}_k) \psi_k - \psi_{k-1}|^2 + |(-1 + i\tilde{A}_k) \psi_k + \psi_{k+1}|^2 \right] \right\} + \frac{I\Phi_0}{2\pi c} \sum \tilde{A}_k. \quad (7)$$

The intuitive meaning of $\tilde{\xi}$ is “the number of consecutive segments over which the order parameter remains approximately uniform.” In numeric calculations $\tilde{\xi}$ has to be of the order of 1; if $\tilde{\xi}$ is too small the discretized model does not represent the physical sample and, if it is too big, the calculation becomes inefficient. Discretization of the local terms in Eq. (6) is quite natural, but discretization of the term with the gradient is somewhat arbitrary. It is tempting to replace the term in square brackets with $|\psi_{k+1} - \psi_{k-1} + 2i\tilde{A}_k\psi_k|^2/2$. Unfortunately, in the limit $N \gg 1$ this form would lead to two separate sublattices (k odd and k even) such that there is no penalty for changing their relative phases; this feature does not represent the original continuous model.

We decompose ψ_k into real variables $\psi_k = u_k + iv_k$. The derivative of the discretized energy with respect to u_k may be written as

$$\frac{\partial G}{\partial u_k} = \frac{Lw_k}{N} \text{Re} \left\{ 2\alpha\psi_k + 2\beta|\psi_k|^2\psi_k + |\alpha|\tilde{\xi}^2 \left[2(1 + \tilde{A}_k^2)\psi_k - (1 + i\tilde{A}_k)\psi_{k+1} - (1 - i\tilde{A}_k)\psi_{k-1} + w_k^{-1} [w_{k-1}(\psi_k - (1 - i\tilde{A}_{k-1})\psi_{k-1}) + w_{k+1}(\psi_k - (1 + i\tilde{A}_{k+1})\psi_{k+1})] \right] \right\}. \quad (8)$$

The derivative with respect to v_k involves the imaginary part of the same expression, which is actually $2\partial G/\partial\psi_k^*$.

The derivative of the energy with respect to \tilde{A}_k is

$$\frac{\partial G}{\partial \tilde{A}_k} = \frac{I\Phi_0}{2\pi c} + \frac{N|\alpha|\xi^2 w_k}{L} [(v_{k+1} - v_{k-1} + 2\tilde{A}_k u_k)u_k - (u_{k+1} - u_{k-1} - 2\tilde{A}_k v_k)v_k]. \quad (9)$$

Noting that the term in square brackets is proportional to a discretized version of the superconducting current density and substituting $|\alpha|\xi^2 = \hbar^2/2m$, Eq. (9) reduces to

$$\frac{\partial G}{\partial \tilde{A}_k} = \frac{I_N \Phi_0}{2\pi c}, \quad (10)$$

where I_N is the normal current along the wire.

C. Evolution equations

Comparison of Ohm's law with Eq. (10) gives the macroscopic equation

$$d\tilde{A}_k/dt = -\Gamma_{A,k} \partial G / \partial \tilde{A}_k, \quad (11)$$

with

$$\Gamma_{A,k} = \frac{4e^2 L}{N\hbar^2 \sigma w_k}. \quad (12)$$

Equation (8) has to be compared with the evolution of the order parameter in a wire [10]. Using superconductor-insulator boundary conditions and our notation, this evolution is given by

$$\gamma\hbar\partial_t\psi = -\{\alpha + \beta|\psi|^2 + |\alpha|\xi^2[(i\partial_s - 2\pi A/\Phi_0)^2 + i(w'(s)/w(s))(i\partial_s - 2\pi A/\Phi_0)]\}\psi, \quad (13)$$

where s denotes the arc length. Assuming that w , ψ and A can be differentiated twice, Eq. (13) is obtained as the limit of

$$du_k/dt = -\Gamma_{\psi,k}\partial G/\partial u_k, \quad (14)$$

and an analogous equation for v_k , with

$$\Gamma_{\psi,k} = \frac{N}{2\gamma\hbar L w_k}. \quad (15)$$

The macroscopic evolution of u_k and v_k can be described by the complex equation $d\psi_k/dt = -2\Gamma_{\psi,k}\partial G/\partial\psi_k^*$.

We close this section with a summary of our numerical algorithm. Let ψ_k and \tilde{A}_k be known at a certain instant. Then, after a time step τ their new values will be

$$\begin{aligned} \psi_k &\leftarrow \psi_k - 2\Gamma_{\psi,k}\tau\frac{\partial G}{\partial\psi_k^*} + \eta_u + i\eta_v \\ \tilde{A}_k &\leftarrow \tilde{A}_k - \Gamma_{A,k}\tau\frac{\partial G}{\partial\tilde{A}_k} + \eta_A, \end{aligned} \quad (16)$$

where η_u , η_v and η_A are random numbers with gaussian distribution, zero average and variances $\langle\eta_u^2\rangle = \langle\eta_v^2\rangle = 2\Gamma_{\psi,k}k_B T\tau$, $\langle\eta_A^2\rangle = 2\Gamma_{A,k}k_B T\tau$, with the derivatives of G given by Eqs. (8)–(9) and the Γ 's given by Eqs. (12) and (15). It should be emphasized that $\Gamma_{A,k}$ and $\Gamma_{\psi,k}$ depend on the length and the cross section of the k^{th} segment.

D. A gauge-invariant method

For a one dimensional wire the electromagnetic potential can be gauged out of the evolution equation by an appropriate transformation. Defining a gauge function

$$\mathcal{U}(s) = \exp\left(\frac{2\pi i}{\Phi_0} \int_0^s A(s')ds'\right) \quad (17)$$

and the gauge-invariant order parameter $\tilde{\psi}(s) = \mathcal{U}(s)\psi(s)$, the term $|(i\nabla - 2\pi\mathbf{A}/\Phi_0)\psi|$ in Eq. (6) reduces to $|d\tilde{\psi}/ds|$. We discretize \mathcal{U} as

$$\mathcal{U}_k = \exp \left(i \sum_{j=1}^{k-1/2} \tilde{A}_j \right), \quad (18)$$

where the sum up to a half-integer number is understood to contain the term \tilde{A}_k , but multiplied by $\frac{1}{2}$. Once \mathcal{U}_k is defined, we can write $\tilde{\psi}_k = \mathcal{U}_k\psi_k$. A discretized version of the energy can then be written as

$$G = \frac{L}{N} \sum \left\{ w_k(\alpha|\tilde{\psi}_k|^2 + \beta|\tilde{\psi}_k|^4/2) + \frac{|\alpha|}{2}\tilde{\xi}^2(w_k + w_{k+1})|\tilde{\psi}_{k+1} - \tilde{\psi}_k|^2 \right\} + \frac{I\Phi_0}{2\pi c} \sum \tilde{A}_k, \quad (19)$$

where w_k is understood as 0 for $k = 0$ and $k = N + 1$.

Although $\tilde{\psi}_k$ is physically more meaningful than ψ_k ($|d\tilde{\psi}/ds|$ is proportional to the velocity), it is not a “canonical” variable, i.e., $d\tilde{\psi}_k/dt \neq -2\Gamma\partial G/\partial\tilde{\psi}_k^*$. Instead, we have

$$\frac{d\tilde{\psi}_k}{dt} = \mathcal{U}_k \frac{d\psi_k}{dt} + i\tilde{\psi}_k \sum_{j=1}^{k-1/2} \frac{\tilde{A}_j}{dt}. \quad (20)$$

Noting that

$$\frac{d\psi_k}{dt} = -2\Gamma_{\psi,k} \frac{\partial G}{\partial\tilde{\psi}_k^*} \frac{\partial\tilde{\psi}_k^*}{\partial\psi_k^*}, \quad (21)$$

the first term in Eq. (20) takes the value $-2\Gamma_{\psi,k}\partial G/\partial\tilde{\psi}_k^*$, i.e., its contribution is what we would obtain if $\tilde{\psi}_k$ were a canonical variable. In order to obtain the evolution of \tilde{A}_j , we express the energy in Eq. (19) in terms of ψ rather than $\tilde{\psi}$ and then use Eq. (11). This gives

$$\frac{d\tilde{A}_j}{dt} = -\Gamma_{A,j} \left(\frac{I\Phi_0}{2\pi c} + \frac{|\alpha|L\tilde{\xi}^2}{2N} \text{Im} \left[(w_{j-1} + w_j)\tilde{\psi}_{j-1}^*\tilde{\psi}_j + (w_j + w_{j+1})\tilde{\psi}_j^*\tilde{\psi}_{j+1} \right] \right), \quad (22)$$

which is the discrete version of Ohm’s law required by Eq. (19). Substituting these results into Eq. (20) we obtain the macroscopic evolution of $\tilde{\psi}$. This evolution can be followed without any knowledge about \tilde{A} .

We investigate now the influence of fluctuations. $\tilde{\psi}_k$ is the same as ψ_k , rotated in the complex plane; therefore, its fluctuations arise from those of ψ_k and from those in the angle of rotation. Since the size of the fluctuations of the real and the imaginary part of ψ_k are

the same and since they are not correlated, their contribution to the fluctuations of $\tilde{\psi}_k$ has the same distribution as $\eta_u + i\eta_v$. The influence of the fluctuations in the angle of rotation can be taken into account as follows. When integrating the evolution of $\tilde{\psi}_k$ in Eq. (20) we require the macroscopic change of \tilde{A}_j , $\tau d\tilde{A}_j/dt$. To this macroscopic change, we have to add the fluctuation of \tilde{A}_j during the period τ , η_A , which is still described by $\langle \eta_A^2 \rangle = 2\Gamma_{A,j}k_B T\tau$.

Our algorithm for the evolution of $\tilde{\psi}_k$ consisted of compound steps. The first stage of a step, that corresponds to the first term in Eq. (20), looks the same as the evolution of ψ_k in Eq. (16), with A_k set to zero. The second stage takes care of the last term in Eq. (20); instead of a standard Euler step we multiply by a phase, i.e.,

$$\tilde{\psi}_k \leftarrow \tilde{\psi}_k \prod_{j=1}^{k-1/2} \exp \left(i \frac{\tilde{A}_j}{dt} \tau + i\eta_{A,j} \right) \quad (23)$$

where the meaning of the upper limit is that the argument of the exponential for $j = k$ is divided by 2. To first order in τ and $\eta_{A,j}$ this method is equivalent to an Euler step, but, since it keeps $|\tilde{\psi}_k|$ unchanged, is numerically more stable.

E. Dimensionless parameters

Besides $\tilde{\xi}$ and \tilde{A} , that were defined before Eq. (7), it will be convenient to define the following dimensionless quantities. $\tilde{\alpha} = \alpha/k_B T$ provides a conveniently normalized value of the condensation energy. $\tilde{L} = L(2mk_B T)^{1/2}/\hbar$ is the length of the wire divided by the “thermal wavelength,” except for a factor $\sqrt{\pi}$. We also define $\tilde{R} = 4e^2\gamma L/\hbar\sigma w_0$, where w_0 is some typical cross section of the wire. For a wire of uniform cross section, \tilde{R} is the normal resistance of the wire multiplied by $2\pi\gamma$ and divided by the quantum of resistance, $h/(2e)^2$. \tilde{R} is proportional to the ratio between the relaxation times of the order parameter and the electromagnetic potential. $\tilde{\tau} = \alpha\tau/\gamma\hbar$ is the effective size of the iteration steps; it is not dictated by the physics of the problem and we expect that, provided that $\tilde{\tau}$ is significantly smaller than 1 and significantly larger than the inverse of the number of iterations, the results should not depend on it. Some additional quantities, which are useful when $\beta \neq 0$, will be defined in Sec. IV C 1.

III. TOY MODELS

In order to test our method, we would like to compare its results against quantities that can be evaluated exactly. For this purpose, the following sections consider simplified models.

A. Uniform \tilde{A}

We drop the last term in Eq. (7), that causes the energy to be unbounded from below, and also set $\beta = 0$, so that the problem becomes linear in the order parameter. In order to keep G bounded from below, we must set $\alpha > 0$. As additional simplifications we will consider a uniform wire $w_k = w_0$ for $k = 1, \dots, N$, and a uniform value $\tilde{A}_k = \tilde{A}$ for all the segments. With these simplifications the energy becomes

$$G = \frac{\alpha L w_0}{N} \sum \left\{ |\psi_k|^2 + \frac{\tilde{\xi}^2}{2} \left[|(1 + i\tilde{A})\psi_k - \psi_{k-1}|^2 + |(-1 + i\tilde{A})\psi_k + \psi_{k+1}|^2 \right] \right\}. \quad (24)$$

We also have to specify boundary conditions at the extremes of the wire. Let us consider periodic boundary conditions, $\psi_0 = \psi_N$, $\psi_{N+1} = \psi_1$.

For a fixed value of \tilde{A} , G can be diagonalized by a Fourier transformation. We define $\varphi_n = N^{-1} \sum \psi_k e^{-2\pi i k n / N}$ and, for simplicity of notation, we will take even values of N . The inverse transformation can be written as

$$\psi_k = \sum_{n=-N/2+1}^{N/2} \varphi_n e^{2\pi i k n / N}. \quad (25)$$

Substituting Eq. (25) into Eq. (24) we obtain

$$G = \alpha L w_0 \sum_{n=-N/2+1}^{N/2} |\varphi_n|^2 \left(1 + \tilde{\xi}^2 [(\tilde{A} + \sin 2\pi n / N)^2 + 4 \sin^4 \pi n / N] \right). \quad (26)$$

The ensemble average of any quantity Q is given by

$$\langle Q \rangle = \int Q(\{\varphi_n\}; \tilde{A}) e^{-G/k_B T} d^2 \varphi_{-N/2+1} \cdots d^2 \varphi_{N/2} d\tilde{A} / \int e^{-G/k_B T} d^2 \varphi_{-N/2+1} \cdots d^2 \varphi_{N/2} d\tilde{A}, \quad (27)$$

where \tilde{A} varies over \mathbf{R} and φ_n over \mathbf{R}^2 . If Q is a polynomial, the integrals over φ_n are easily evaluated. For example, the denominator in Eq. (27) (the partition function) is

$$Z = \int_{-\infty}^{\infty} \frac{(\pi k_B T / \alpha L w_0)^N d\tilde{A}}{(1 + \tilde{\xi}^2(\tilde{A}^2 + 4)) \prod_{n=1-N/2}^{N/2-1} (1 + \tilde{\xi}^2[(\tilde{A} + \sin 2\pi n / N)^2 + 4 \sin^4 \pi n / N])}. \quad (28)$$

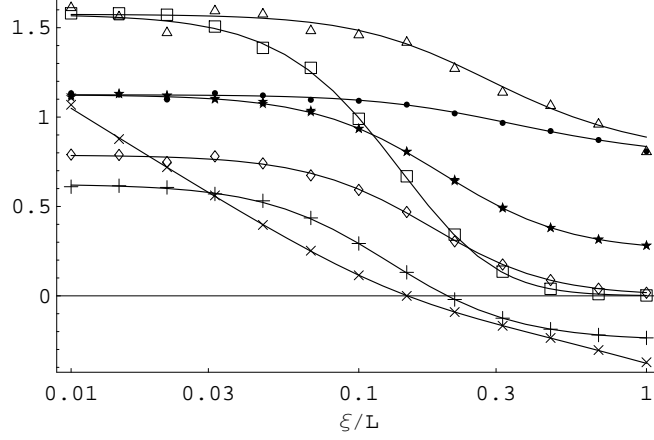


FIG. 1: Averages of several quantities, as functions of the coherence length. The symbols correspond to values calculated using our method and the lines are ensemble averages. The parameters used in the calculation were $N = 4$, $\tilde{\tau} = 3 \times 10^{-5}$, $\tilde{R} = 16000$, $N_{\text{av}} = 2 \times 10^8$, $N_{\text{relax}} = 6 \times 10^7$. The parameter $\tilde{\alpha}$ factors out. $\bullet \tilde{\alpha} L w_0 \langle |\varphi_0|^2 \rangle + 0.25$ (the constant 0.25 was added for visibility); $\star \tilde{\alpha} L w_0 \langle |\varphi_{-1}|^2 \rangle + 0.25$ and $\tilde{\alpha} L w_0 \langle |\varphi_1|^2 \rangle + 0.25$; $+ \tilde{\alpha} L w_0 \langle |\varphi_2|^2 \rangle - 0.25$; $\triangle (\tilde{\alpha} L w_0)^2 \langle |\varphi_0|^4 \rangle$; $\square (\tilde{\alpha} L w_0)^2 \langle |\varphi_1|^4 \rangle$; $\diamond (\tilde{\alpha} L w_0)^2 \langle |\varphi_0|^2 |\varphi_1|^2 \rangle$; $\times 0.5 \log_{10} \langle \tilde{A}^2 \rangle$.

This last integral may be either evaluated numerically or collecting the residues at $\tilde{A} = \sin 2\pi n/N + i(\tilde{\xi}^{-2} + 4 \sin^4 \pi n/N)^{1/2}$.

Note that, since the dependence on \tilde{A} factors out in the integrand of Eq. (28), it contributes just a multiplicative constant to the partition function. Therefore, \tilde{A} is a degree of freedom that makes no contribution to the heat capacity. For the same reason, the expectation value for any function of \tilde{A} is independent of the temperature.

In our calculations using algorithm (16) we started from $u_k = v_k = \tilde{A} = 0$ and let these variables build up from fluctuations. We performed N_{relax} iterations to achieve a “typical” situation and then averaged the quantities of interest during N_{av} additional iterations.

Figure 1 compares the averages of several quantities, as obtained with our method for $N = 4$, with those expected from Eq. (27), for a wide range of values of ξ/L . If the fluctuations of \tilde{A} are ignored, we obtain the results in Fig. 2. As expected, ignoring the fluctuations of \tilde{A} yields a variance of \tilde{A} (not shown in the graph) that is much lower than its ensemble value, but we see in Fig. 2 that also the averages of quantities that do not directly involve \tilde{A} turn out to be incorrect. Due to the inversion symmetry of this model, averages such as $\langle |\varphi_{-n}|^2 \rangle$ and $\langle |\varphi_n|^2 \rangle$ coincide.

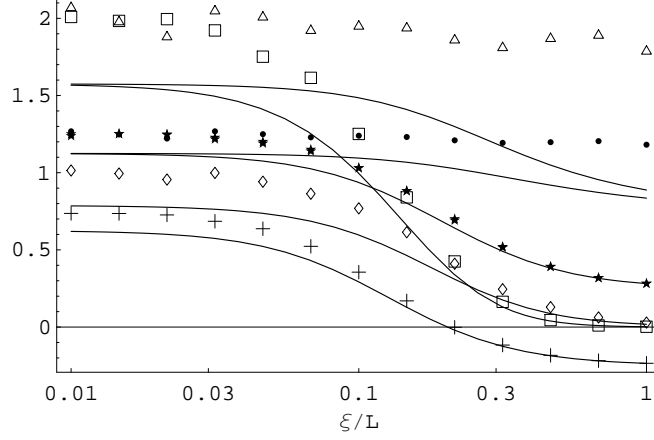


FIG. 2: Same as Fig. 1, but fluctuations of \tilde{A} were ignored.

Figure 3 compares the averages $\langle |\varphi_n|^2 \rangle$ obtained with our method with those expected from Eq. (27) for $N = 10$ and Fig. 4 repeats the comparison while ignoring fluctuations of \tilde{A} . We see again that the symbols in Fig. 4 deviate from Eq. (27), but this time the disagreement is smaller than in the case $N = 4$. The reason is that the variable \tilde{A} is driven by the other variables u_i and v_i ; when ξ/L is sufficiently large, the variance of \tilde{A} is practically independent of whether or not its fluctuations are considered. This is a feature of our toy model, in which there are $2N$ degrees of freedom for the order parameter and only one for \tilde{A} ; in the original model with N degrees of freedom for \tilde{A}_i the influence of the fluctuations of the electromagnetic field should not decrease with N .

B. Gauge-invariant formalism

We still take $I = \beta = 0$ and uniform cross section $w_k = w_0$, but use of the formalism developed in Sec. IID enables us to release the requirement of uniform \tilde{A} . We consider two boundary conditions. One of them is $\tilde{\psi}(0) = \tilde{\psi}(L) = 0$, which corresponds to contacts with a conductor that strongly suppresses superconductivity. In a discrete model, these conditions are approximated by $\tilde{\psi}_0 = -\tilde{\psi}_1$ and $\tilde{\psi}_{N+1} = -\tilde{\psi}_N$. In this case we write

$$\tilde{\psi}_k = \sum_{n=1}^N \varphi_n^s \sin \frac{n(k-1/2)\pi}{N} \quad (29)$$

with

$$\varphi_n^s = \frac{2 - \delta_{nN}}{N} \sum_{k=1}^N \tilde{\psi}_k \sin \frac{n(k-1/2)\pi}{N}, \quad (30)$$

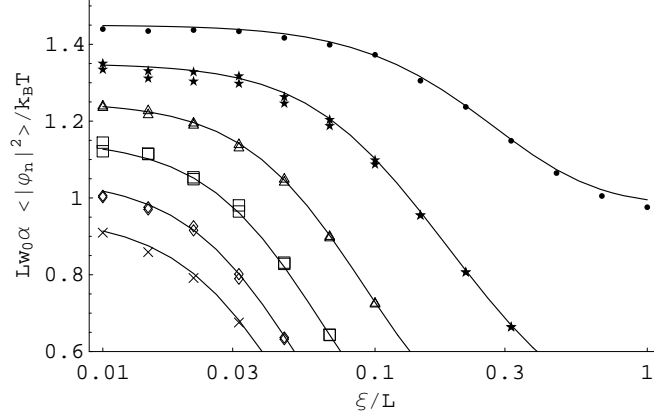


FIG. 3: Variances of the Fourier components of the order parameter, as functions of the coherence length, for the case of 10 segments. The curve for $n = 5$ sits at its true position; for visibility, the other curves have been raised by $(5 - |n|)/10$. Besides N , the parameters are the same as in Fig. 1.
 \bullet $n = 0$; \star $n = \pm 1$; \triangle $n = \pm 2$; \square $n = \pm 3$; \diamond $n = \pm 4$; \times $n = 5$.

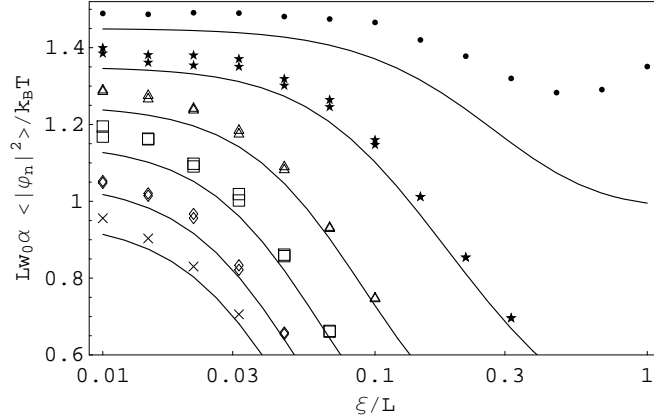


FIG. 4: Same as Fig. 3, but fluctuations of \tilde{A} were ignored. The vertical scale has been expanded in order to emphasize the disagreement.

where δ is Kroneker's symbol. Expression (19) then assumes the diagonal form

$$G = \alpha L w_0 \sum_{n=1}^N (1 + \delta_{nN}) |\varphi_n^s|^2 \left(\frac{1}{2} + 2\tilde{\xi}^2 \sin^2 \frac{n\pi}{2N} \right). \quad (31)$$

The other boundary condition we consider is that in which $d\tilde{\psi}/ds$ vanishes, which corresponds to contacts with an insulator. In a discrete model, we require $\tilde{\psi}_0 = \tilde{\psi}_1$ and

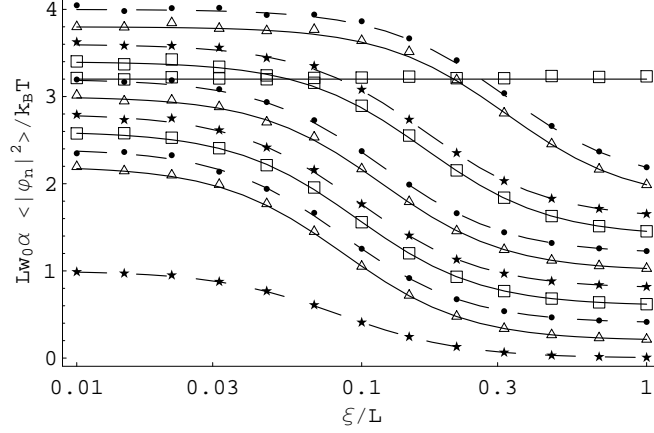


FIG. 5: Variances of the Fourier components φ_n^s and φ_n^c of the gauge-invariant order parameter $\tilde{\psi}$, for $N = 6$. The dashed lines describe $\langle |\varphi_n^s|^2 \rangle$ according to Eq. (31) ($\tilde{\psi} = 0$ at the boundaries), and have been raised by $0.4(6 - n)$. The solid lines describe $\langle |\varphi_n^c|^2 \rangle$ according to Eq. (34) ($d\tilde{\psi}/ds = 0$ at the boundaries), and have been raised by $0.4(5.5 - n)$. Note that $\langle |\varphi_0^c|^2 \rangle$ does not depend on ξ . The symbols describe the values obtained using the method developed in Sec. IID. \bullet $\langle |\varphi_n^s|^2 \rangle$, n odd; \star $\langle |\varphi_n^s|^2 \rangle$, n even; \triangle $\langle |\varphi_n^c|^2 \rangle$, n odd; \square $\langle |\varphi_n^c|^2 \rangle$, n even. Besides $N = 6$ and $\tilde{\tau} = 10^{-5}$, the parameters are the same as in Fig. 1.

$\tilde{\psi}_{N+1} = \tilde{\psi}_N$. In this case we write

$$\tilde{\psi}_k = \sum_{n=0}^{N-1} \varphi_n^c \cos \frac{n(k-1/2)\pi}{N} \quad (32)$$

with

$$\varphi_n^c = \frac{2 - \delta_{n0}}{N} \sum_{k=1}^N \tilde{\psi}_k \cos \frac{n(k-1/2)\pi}{N} \quad (33)$$

and Eq. (19) reduces to

$$G = \alpha L w_0 \left\{ |\varphi_0^c|^2 + \sum_{n=1}^{N-1} |\varphi_n^c|^2 \left(\frac{1}{2} + 2\tilde{\xi}^2 \sin^2 \frac{n\pi}{2N} \right) \right\}. \quad (34)$$

Figures 5 and 6 show values of $\langle |\varphi_n^s|^2 \rangle$ and $\langle |\varphi_n^c|^2 \rangle$ obtained from Eqs. (30) and (33) after following the evolution of $\tilde{\psi}$ according to Sec. IID. We see that, in spite of the fact that the vector potential \tilde{A}_k has been gauged out and the macroscopic evolution of $\tilde{\psi}$ can be described in closed form by means of Eqs. (20) and (22), the fluctuations of \tilde{A}_k still remain essential.

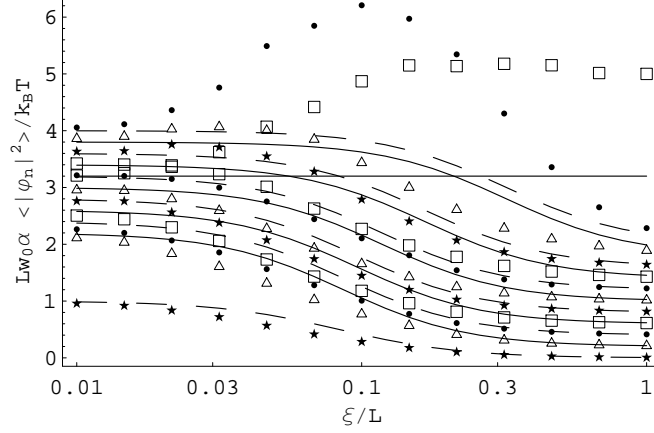


FIG. 6: Same as Fig. 5, but fluctuations of \tilde{A} were ignored.

C. The continuous limit

We consider now the limit $N \rightarrow \infty$. In this limit $\Gamma_A \rightarrow 0$, and we might expect that the fluctuations of \tilde{A}_k become unimportant. As in the previous section, we drop the nonlinear term, take a uniform cross section, and use the gauge-invariant order parameter $\tilde{\psi}$. This time we will consider the periodic boundary condition $\tilde{\psi}_{N+1} = \tilde{\psi}_1$, which physically corresponds to a ring that encloses a magnetic flux that equals an integer number of quanta. The case of a ring that encloses a non-integer flux will be considered elsewhere. For this boundary condition we cannot take $I = 0$; instead, I becomes a Lagrange multiplier. Numerically, the effect of this current amounts to the subtraction of a uniform term from every \tilde{A}_k , so that $\sum \tilde{A}_k(t)$ remains constant.

Since $d\tilde{\psi}/dt$ diverges in the limit $N \rightarrow \infty$, direct application of Euler iterations would require prohibitively small time steps for $N \gg 1$. We therefore treat the leading term separately. Regarding $\boldsymbol{\psi} = (\tilde{\psi}_1, \dots, \tilde{\psi}_N)$ as a vector, we have to leading term

$$\frac{d\boldsymbol{\psi}}{dt} = \mathbf{M}\boldsymbol{\psi}, \quad (35)$$

where the matrix \mathbf{M} has the elements $-2\alpha\tilde{\xi}^2/\gamma\hbar$ along the diagonal, $\alpha\tilde{\xi}^2/\gamma\hbar$ when the column and the row number differ by 1 (modulo N), and zeros everywhere else. Ignoring the other contributions, Eq. (35) can be integrated to give

$$\boldsymbol{\psi}(t + \tau) = \exp(\mathbf{M}\tau)\boldsymbol{\psi}(t). \quad (36)$$

\mathbf{M} has eigenvalues that are either negative or zero, so that the largest eigenvalue of $\exp(\mathbf{M}\tau)$ is 1.

TABLE I: $10^4 \tilde{\alpha} L w_0 \langle |\tilde{\varphi}_n|^2 \rangle$ for several values of the number of elements N and the wave number n . We have taken a coherence length equal to the length of the sample, and the other parameters are as in Fig. 1.

	$N = 8$			$N = 16$			$N = 32$			$N = 64$		
n	a	b	c	a	b	c	a	b	c	a	b	c
0	10000	9994	30533	10000	10771	47427	10000	11249	71936	10000	9750	1.03×10^5
1	256	258	137	250	251	128	248	250	125	247	247	122
2	78	78	49	66	66	37	64	63	34	63	63	33
3	46	46	37	32	32	20	29	29	17	28	28	16
4	39	39	39	19	20	14	17	17	10	16	16	9

^aStatistical average

^bEvaluated with the method of Sec. III C

^cMethod of Sec. III C, without fluctuations in \tilde{A}_k

We can therefore follow the evolution of $\tilde{\psi}_k$ by means of steps that consist of three stages. The first stage is described by Eq. (36) and the other two are as in the previous section. When considering the contribution of the first term in Eq. (20), the leading term is now dropped. The matrix $\exp(\mathbf{M}\tau)$ is the same for every step, so that it has to be calculated just once.

Defining $\tilde{\varphi}_n = N^{-1} \sum \tilde{\psi}_k e^{-2\pi i k n / N}$, the statistical average of $\langle |\tilde{\varphi}_n|^2 \rangle$ can be obtained by setting $\tilde{A} \rightarrow 0$ in Eq. (26). From here we obtain $\langle |\tilde{\varphi}_n|^2 \rangle = k_B T / \alpha L w_0 (1 + 4\tilde{\xi}^2 \sin^2(n\pi/N))$. Table I compares this statistical average with the values obtained with and without fluctuations of \tilde{A}_k for several values of N and n . For the parameters considered, we see that the larger the number of elements into which we divide the sample, the more severe the error of the results obtained when the fluctuations of \tilde{A}_k are ignored.

D. Average supercurrent

We would like to determine a characteristic size for the supercurrent. We consider again a wire with uniform cross section with periodic boundary conditions. The average of the

supercurrent along the wire is

$$I_{\text{SC}} = \frac{4e\alpha\tilde{\xi}^2 L w_0}{\hbar N^2} \sum_{j=1}^N \text{Im} \left[\tilde{\psi}_j^* \tilde{\psi}_{j-1} \right] , \quad (37)$$

which can also be written as

$$I_{\text{SC}} = -\frac{4e\alpha\tilde{\xi}^2 L w_0}{\hbar N} \sum_{n=0}^{N-1} |\tilde{\varphi}_n|^2 \sin \frac{2\pi n}{N} . \quad (38)$$

The ensemble average of I_{SC} is zero. Its variance is obtained from the square of Eq. (38),

$$I_{\text{SC}}^2 = \frac{(4e\alpha\tilde{\xi}^2 L w_0)^2}{(\hbar N)^2} \sum_{n,n'} |\tilde{\varphi}_n|^2 |\tilde{\varphi}_{n'}|^2 \sin \frac{2\pi n}{N} \sin \frac{2\pi n'}{N} . \quad (39)$$

The expression for the variance is simplified by subtraction of the null quantity $\langle I_{\text{SC}} \rangle^2$ and noting that for $n \neq n'$ $\langle |\tilde{\varphi}_n|^2 |\tilde{\varphi}_{n'}|^2 \rangle = \langle |\tilde{\varphi}_n|^2 \rangle \langle |\tilde{\varphi}_{n'}|^2 \rangle$, whereas $\langle |\tilde{\varphi}_n|^4 \rangle = 2 \langle |\tilde{\varphi}_n|^2 \rangle^2$. We obtain

$$\langle I_{\text{SC}}^2 \rangle = \frac{(4e\tilde{\xi}^2 k_B T)^2}{(\hbar N)^2} \sum_{n=0}^{N-1} \frac{\sin^2(2\pi n/N)}{(1 + 4\tilde{\xi}^2 \sin^2(\pi n/N))^2} . \quad (40)$$

For $N \gg 1$, the sum can be replaced with an integral; if in addition we assume $\tilde{\xi} \gg 1$ and keep only the leading term, Eq. (40) becomes

$$\langle I_{\text{SC}}^2 \rangle = \frac{4e^2 k_B^2 T^2 \tilde{\xi}}{\hbar^2 L} . \quad (41)$$

E. Nonuniform ring

We finally consider a case with nonuniform cross section. We use the gauge-invariant description in Eq. (19), with $\beta = 0$ and consider a ring with just $N = 3$ elements. For simplicity, we also take $\xi = L/3$. We take periodic boundary conditions, as in Sec. III C. We denote the cross sections by $w_1 = \mu w_0$ and $w_2 = w_3 = w_0$. This is an artificial model and clearly we cannot regard its boundary as a smooth surface, but the important feature for the present purpose is that it is a self-consistent model.

The energy can be diagonalized by a linear transformation $\tilde{\psi}_1 = \varphi_1 + \varphi_2 + \varphi_3$, $\tilde{\psi}_{2,3} = \varphi_1 - (\mu/2)(\varphi_2 + \varphi_3) \pm \nu(\varphi_2 - \varphi_3)$, with $\nu = \frac{1}{2}((4 + 12\mu + 7\mu^2 + \mu^3)/(7 + \mu))^{1/2}$. This transformation gives $G = (\alpha L w_0/6)(2 + \mu)(2|\varphi_1|^2 + (2 + 5\mu + \mu^2)(|\varphi_2|^2 + |\varphi_3|^2))$.

As in Sec. III C, the current becomes a Lagrange multiplier. Since $\Gamma_{A,k} \propto w_k^{-1}$, this time we have to subtract a uniform term from every $w_k \tilde{A}_k$ in order to keep a constant value of $\sum \tilde{A}_k$.

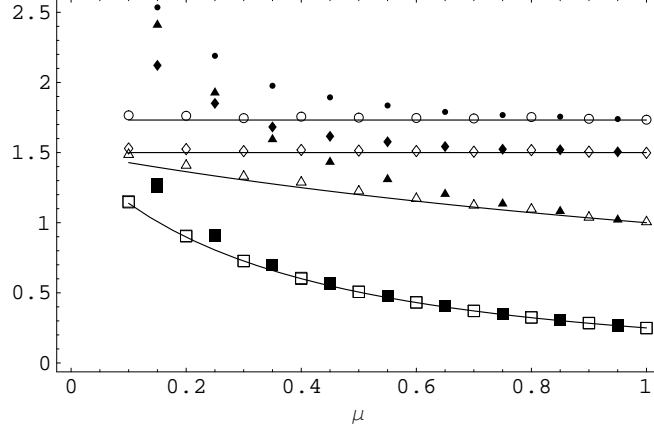


FIG. 7: Statistical averages of several fluctuating quantities as functions of uniformity. For a ring with uniform cross section, $\mu = 1$. The lines were obtained using statistical mechanics, the empty symbols were evaluated using fluctuations with the sizes dictated by Eqs. (12) and (15) and the filled symbols were evaluated using fluctuations of the same size for the three elements. $\triangle \tilde{\alpha}Lw_0\langle|\varphi_1|^2\rangle$; $\square \tilde{\alpha}Lw_0\langle|\varphi_{2,3}|^2\rangle$ ($\varphi_{1,2,3}$ as defined in Sec. III E); $\diamond \langle G\rangle/2k_BT$; $\circ (\langle G^2\rangle)^{1/2}/2k_BT$. Besides $N = 3$ and $\xi = \frac{L}{3}$, the parameters are the same as in Fig. 1.

Figure 7 shows the statistical averages of $|\varphi_{1,2,3}|^2$ and of some powers of the energy that are obtained for this model using the method developed in Sec. II. For comparison, we also evaluated these averages using fluctuation sizes that are independent of the local cross section; for the purpose of this comparison we replaced w_k in Eq. (12) and Eq. (15) with the geometric average of the cross section, $\mu^{1/3}w_0$.

F. Paraconductivity under constant electric field

Tucker and Halperin [14] evaluated the supercurrent along a thin uniform wire when a longitudinal electric field is applied. The strongest assumption of their model is that the electric field remains constant in time and position, and is not influenced by ψ . An unphysical feature of this model is that the total current is not uniform along the wire. The supercurrent is defined by its spatial average, as in Eq. (37). An additional assumption was that the length of the wire is infinite. The main effort of Ref. [14] was focused on the

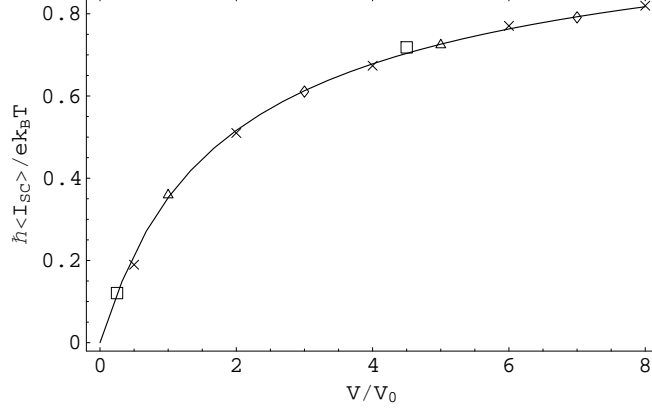


FIG. 8: Average of the superconducting current as a function of the applied voltage under the assumption that the electric field is constant and uniform, in spite of the fluctuations of the superconducting order parameter. The line corresponds to Eq. (42). In all cases $\tilde{\tau} = 3 \times 10^{-5}$, $\tilde{\xi} = 21$ and, unless stated otherwise, $N_{\text{av}} = 2 \times 10^8$, $N_{\text{relax}} = 6 \times 10^7$ and $\tilde{\alpha} = 10$. \triangle $\xi = L$, $\tilde{\alpha} = 4$; \square $\xi = 0.3L$; \diamond $\xi = L$; \times $\xi = 3L$, $N_{\text{av}} = 3 \times 10^8$, $N_{\text{relax}} = 9 \times 10^7$.

influence of the term $\beta|\tilde{\psi}|^4$ in Eq. (6), but at this stage we keep $\beta = 0$. Their result was

$$I_{\text{SC}} = \frac{ek_B T}{\sqrt{\pi}\hbar} \int_0^\infty dy y^{1/2} \exp \left[- \left(\frac{V_0}{V} \right)^{2/3} y - \frac{y^3}{12} \right], \quad (42)$$

where V is the applied voltage and $V_0 = \alpha L / \gamma e \xi$. I_{SC} is an increasing function of V ; for $V \gg V_0$, I_{SC} approaches $2ek_B T / \sqrt{3}\hbar = 1.15ek_B T / \hbar$.

In order to reproduce this model, we follow just the evolution of $\tilde{\psi}_k$, whereas $\tilde{A}_k(t)$ follows from $d\tilde{A}_k/dt = -2eV/N\hbar$. We take periodic boundary conditions for ψ , i.e. $\tilde{\psi}_{N+1} = \exp(-2ieVt/\hbar)\tilde{\psi}_1$, and the condition of infinite length requires $L \gg \xi$. The results are shown in Fig. 8 for several cases in the range $0.3 \leq \xi \leq 3L$. There is good agreement with the prediction of Ref. [14] but, surprisingly, the requirement of large L seems to be unnecessary.

IV. APPLICATION—PARACONDUCTIVITY

A. Voltage-current characteristic of a uniform wire

We are now in a position that enables us to evaluate self-consistently the average current $\langle I \rangle$ along a superconducting wire when a fixed voltage V is applied. The procedure is similar to that of Sec. III F, but this time the evolution of \tilde{A}_k is given by Eq. (16). The instantaneous

total current I has to be such that in every step $\sum \tilde{A}_k$ decreases by $2eV\tau/\hbar$. $\langle I \rangle$ is obtained as the average of I over N_{av} iteration steps.

The dashed lines in Fig. 9 show the values obtained for $\langle I \rangle(V)$ in the range $10^{-1} \lesssim I\hbar/ek_BT \lesssim 10^{3/2}$ and $40 \leq \tilde{R} \leq 25000$. For $\tilde{R} = 40$ these values are scarcely below the currents that would be present in a normal material (in a logarithmic scale); this means that supercurrents are small compared to the normal currents. For larger values of \tilde{R} , Ohm's law is approached in the large current extreme, whereas in the low current extreme $\langle I \rangle$ is not proportional to V . We may expect that $\langle I \rangle$ could become proportional to V for still lower currents, but Eq. (41) predicts fluctuations of $I_{\text{SC}}\hbar/ek_BT$ of the order of $\sqrt{\xi/L}$ for a single step. Since the number of independent values of I_{SC} is of the order of $N_{\text{av}}\tilde{\tau} \sim 10^3$, we should at best expect $\langle I \rangle\hbar/ek_BT$ to be accurate to the order of 10^{-2} . Therefore, we did not attempt to evaluate $\langle I \rangle$ for lower currents.

Another experimental situation is prescribed by keeping a fixed current I . In this case we are interested in the average value of the voltage. The evolution of $\tilde{\psi}$ and \tilde{A} is the same as in Sec. IIIC, except for an additional term $\tilde{R}\tilde{\tau}\hbar I/2N\tilde{\alpha}ek_BT$ in the increment of each \tilde{A}_k in every step. The boundary conditions are dictated by the experimental setup; in the absence of experimental details we shall just assume that the coupling between ψ_1 and ψ_0 (and between ψ_N and ψ_{N+1}) can be neglected. In order to avoid a significant influence of the boundary conditions at the ‘‘contacts,’’ we adopted a ‘‘four-probe technique,’’ i.e., the voltage was measured between the segments $1 + N_{\text{cont}}$ and $N - N_{\text{cont}}$ and the result was multiplied by $N/(N - 2N_{\text{cont}})$.

The average voltage drop $\langle V \rangle$ is given by

$$\frac{\gamma e \langle V \rangle}{k_BT} = -\frac{N}{N - 2N_{\text{cont}}} \frac{\tilde{\alpha}}{2N_{\text{av}}\tilde{\tau}} \sum \Delta \tilde{A}_k, \quad (43)$$

where $\Delta \tilde{A}_k$ is the increment of \tilde{A}_k in a step and the sum is over the segments $1 + N_{\text{cont}} \leq k \leq N - N_{\text{cont}}$ and also over the N_{av} iteration steps.

The continuous lines in Fig. 9 show our results for $\langle V \rangle(I)$. For large and intermediate currents $\langle V \rangle(I)$ coincides with $\langle I \rangle(V)$ in the scale of the graph, but for low currents we see that they are different curves. This difference might arise from the different boundary conditions, but could also be a matter of principle, since a situation in which I is kept fixed and V fluctuates is not necessarily equivalent to a situation in which V is kept fixed and I fluctuates. This time we do reach a small current regime where $\langle V \rangle$ is proportional to I ,

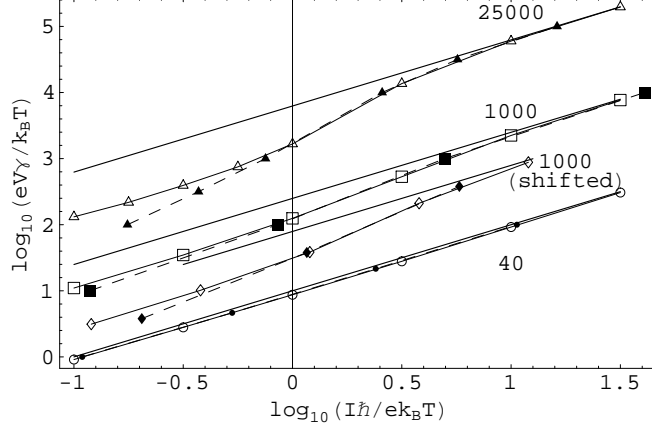


FIG. 9: Voltage-current characteristic. Filled symbols (dashing lines) stand for $\langle I \rangle(V)$ and empty symbols (continuous lines) for $\langle V \rangle(I)$. The straight lines correspond to Ohm's law in the normal state. Unless stated otherwise, $N = 21$, $N_{\text{cont}} = 3$, $N_{\text{av}} = 2 \times 10^8$, $N_{\text{relax}} = 6 \times 10^7$, $\tilde{\alpha} = 10$, $\xi = L/\sqrt{10}$ and $\tilde{\tau} = 10^{-5}$. The values of \tilde{R} are marked next to the curves in the large-current regime. The lines with the rhombs correspond to $\tilde{R} = 1000$ and $\tilde{\alpha} = 3$; for visibility, they have been lowered by half a unit. For $\tilde{R} = 25000$, several points of $\langle I \rangle(V)$ were evaluated using $\tilde{\tau} = 3 \times 10^{-5}$ and several points of $\langle V \rangle(I)$ were evaluated using $\tilde{\tau} = 3 \times 10^{-6}$, $N_{\text{av}} = 10^8$, $N_{\text{relax}} = 3 \times 10^7$; these changes of computational parameters do not produce noticeable changes in this figure.

with an effective resistance that is smaller than $L/w_0\sigma$.

B. Low current limit

Let us denote by σ' the contribution of the supercurrent to the electric conductivity. Taking the limit $V \rightarrow 0$ in Eq. (42) we obtain

$$\sigma' = \sigma \tilde{R} \xi / 8 \tilde{\alpha} L. \quad (44)$$

This result was initially obtained by Aslamazov and Larkin [15] and the value of σ' according to Eq. (44) will be denoted by σ_{AL} . It can also be written as

$$\sigma_{\text{AL}} = \tilde{R} \sigma \mathbb{L}^2 (\xi/2L)^3 = \tilde{R} \sigma / 8 \tilde{\alpha}^{3/2} \mathbb{L} = K \epsilon^{-3/2}, \quad (45)$$

where $\epsilon = (T - T_c)/T_c$, T_c is the critical temperature and $K = \pi e^2 \xi(0)/16 \hbar w_0$. The last form of Eq. (45) neglects terms of order $\epsilon^{-1/2}$ and assumes $\alpha = 8 k_B (T - T_c) \gamma / \pi$.

We will now evaluate σ' taking the electromagnetic fluctuations into account. This will be done by fixing a small current I , evaluating the average voltage $\langle V \rangle$ as discussed in the previous section, and then σ' will be given by

$$\frac{\sigma'}{\sigma} = \frac{\tilde{R}\hbar I / ek_B T}{4\gamma e \langle V \rangle / k_B T} - 1. \quad (46)$$

The choice of I as the nonfluctuating quantity is based both on Fig. 9 and on the fact that most experiments are performed under this condition.

Let us now discuss the size of the parameters we should use. I has to be sufficiently small in order to yield a voltage proportional to it. Our requirement was $I_{\text{SC}} \lesssim 0.1ek_B T/\hbar$. This value was inspired by Figs. 8 and 9 and is in agreement with experiments [16, 17, 18], that required $I \lesssim 3ek_B T/\hbar$. For experiments that used larger currents, the conductivity was current dependent in the interesting range [19]. Our requirement is translated into the condition $I \lesssim 0.1(1 + \sigma/\sigma')ek_B T/\hbar$. Since σ' was not known in advance, we used $I = 0.1(1 + \sigma/\sigma_{\text{AL}})ek_B T/\hbar$, which turned out to be appropriate in all cases. In several cases we doubled I and verified that $\langle V \rangle$ was indeed doubled.

We also have to choose the value of $\tilde{\tau}$. For the validity of the algorithm (16) we require $\tau \ll k_B T / \Gamma_\psi (\partial G / \partial u_k)^2$. We make the estimates $\partial G / \partial u_k \sim \alpha w_0 L \tilde{\xi}^2 |\psi_k| / N$ and $|\psi_k| \sim \sqrt{N / \tilde{\alpha} w_0 L}$. On the other hand, the fluctuations of I_{SC} , that were estimated in Sec. IV A, have to be small compared to $\langle I_{\text{SC}} \rangle$. Therefore, $\tilde{\tau}$ has to be in the range

$$400\xi / N_{\text{av}} L \ll \tilde{\tau} \ll \tilde{\xi}^{-4}. \quad (47)$$

Similarly, we require $\tau \ll k_B T / \Gamma_A (\partial G / \partial \tilde{A}_k)^2$ and $\langle I_{\text{SC}} \rangle$ has to be large compared to the Johnson noise. From here we obtain

$$800\tilde{\alpha} / N_{\text{av}} \tilde{R} \ll \tilde{\tau} \ll N\tilde{\alpha} / \tilde{R} \tilde{\xi}^4. \quad (48)$$

In addition, we require $N_{\text{relax}} \tilde{\tau} \gg 1$.

Figure 10 shows the results obtained for σ' , for several values of \tilde{R} and ξ/L , while $\tilde{\alpha}$ is varied over typically four orders of magnitude. Most of the results sit on a universal curve. The line in the graph is

$$\sigma' / \sigma = ((\sigma_{\text{AL}} / \sigma)^{-4/5} + (4/5)(\sigma_{\text{AL}} / \sigma)^{-1/8})^{-5/4} \quad (49)$$

and seems to fit the results reasonably well in this range. The results for $\xi = 0.3L$ are too high. We suspect that for this large ξ/L ratio the conductivity is influenced by the boundary

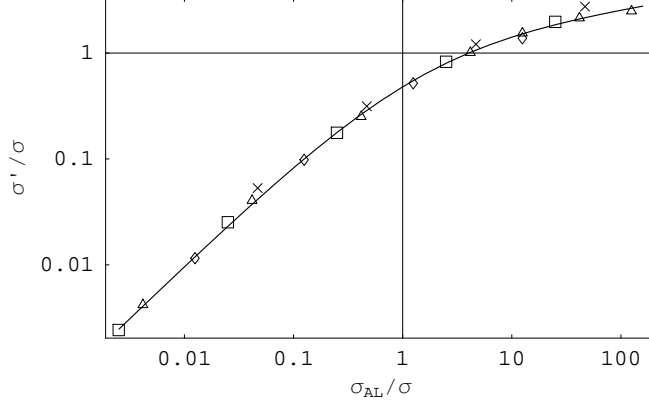


FIG. 10: Superconducting contribution to the electric conductivity, evaluated as described in Sec. IV B and displayed as a function of the contribution that would be obtained according to Eq. (44). The line is an empiric function. In all cases $N_{\text{av}} = 2 \times 10^8$ and $N_{\text{relax}} = 6 \times 10^7$. For $\sigma_{\text{AL}} < 10\sigma$, $\tilde{\tau} = 0.003\tilde{\alpha}/\tilde{R}$; otherwise, $\tilde{\tau} = 0.03\tilde{\alpha}/\tilde{R}$. \triangle $\tilde{R} = 5000$, $\xi = 0.2L$, $N = 14$, $N_{\text{cont}} = 2$; \square $\tilde{R} = 20$, $\xi = 0.2L$, $N = 14$, $N_{\text{cont}} = 2$; \diamond $\tilde{R} = 100$, $\xi = 0.1L$, $N = 28$, $N_{\text{cont}} = 4$; \times $\tilde{R} = 5000$, $\xi = 0.3L$, $N = 14$, $N_{\text{cont}} = 3$.

conditions; it is known that when ξ is of the order of the length of the wire, qualitatively different behavior is obtained [20].

C. Inclusion of the nonlinear term

Until now we have neglected the term with higher order in ψ_k . This can be done for temperatures that are sufficiently above the critical temperature. We are now interested in the region close or below the critical temperature and we therefore set $\beta \neq 0$. Except for the general treatment in Sec. IV C 1, this section will consider a wire with uniform cross section w_0 . In the general case, w_0 stands for a typical cross section.

1. Numeric considerations

We start by defining some useful quantities. $\bar{\psi}$ and ξ_β are defined by requiring $\beta\bar{\psi}^4 w_0 \xi_\beta = k_B T$ and $\beta\bar{\psi}^2 \xi_\beta^2 = \hbar^2/2m$. The implication of this requirement is that $\bar{\psi}$ will be an estimate of the size of the order parameter at the critical temperature, and ξ_β will be an estimate of

the coherence length at this temperature. Solving these two equations gives

$$\bar{\psi} = (2mk_B^2 T^2 / \beta \hbar^2 w_0^2)^{1/6} , \quad (50)$$

$$\xi_\beta = (\hbar^4 w_0 / 4\beta m^2 k_B T)^{1/3} . \quad (51)$$

In terms of more directly measurable quantities we can write

$$\xi_\beta = (w_0 \Phi_0^2 / 32\pi^3 \kappa^2 k_B T)^{1/3} , \quad (52)$$

where κ is the Ginzburg–Landau parameter; for a wire of cross section $w_0 \sim 10^{-11} \text{ cm}^2$, critical temperature $T \sim 1 \text{ K}$ and $\kappa \sim 0.1$, $\xi_\beta \sim 7 \times 10^{-4} \text{ cm}$. We also define the normalized order parameter $\psi_{\beta k} = \psi_k / \bar{\psi}$ (and similarly, $\tilde{\psi}_{\beta k} = \tilde{\psi}_k / \bar{\psi}$), the normalized step size $\tilde{\tau}_\beta = \tau \beta \bar{\psi}^2 / \gamma \hbar$ and the ratio $\alpha' = \alpha / \beta \bar{\psi}^2 = \tilde{\alpha} (\xi_\beta \mathbf{L} / L)^2$; if α is a perfectly linear function of the temperature, then $\alpha' = (\xi_\beta / \xi(0))^2 \epsilon$.

With these notations, the “macroscopic” increments of $\tilde{\psi}_{\beta k}$ and \tilde{A}_k during a time step τ are

$$\begin{aligned} \Delta_{\text{mac}} \tilde{\psi}_{\beta k} = & -\tilde{\tau}_\beta [(\alpha' + |\tilde{\psi}_{\beta k}|^2) \tilde{\psi}_{\beta k} + (N \xi_\beta / L)^2 (2w_k)^{-1} \\ & [(w_k + w_{k+1})(\tilde{\psi}_{\beta k} - \tilde{\psi}_{\beta k+1}) + (w_k + w_{k-1})(\tilde{\psi}_{\beta k} - \tilde{\psi}_{\beta k-1})]] , \end{aligned} \quad (53)$$

$$\begin{aligned} \Delta_{\text{mac}} \tilde{A}_k = & -(\tilde{\tau}_\beta \tilde{R} / 2w_k) (\xi_\beta \mathbf{L} / L)^2 [(w_0 / N)(I \hbar / e k_B T) + \\ & (\xi_\beta / L) \text{Im}[(w_{k-1} + w_k) \tilde{\psi}_{\beta k-1}^* \tilde{\psi}_{\beta k} + (w_k + w_{k+1}) \tilde{\psi}_{\beta k}^* \tilde{\psi}_{\beta k+1}]] . \end{aligned} \quad (54)$$

The fluctuations in the increment of \tilde{A}_k have a variance $2\tilde{R}\tilde{\tau}_\beta (w_0 / N w_k) (\xi_\beta \mathbf{L} / L)^2$; the fluctuations of $\tilde{\psi}_{\beta k}$ are taken into account by adding to the real and to the imaginary part terms with variance $N\tilde{\tau}_\beta w_0 \xi_\beta / w_k L$ and then modifying the phase according to Eq. (23).

As in the previous section, we investigate the range of admissible values for $\tilde{\tau}_\beta$. Our analysis is similar to that leading to Eqs. (47)-(48), but now we use the estimate $|\psi_k| \sim \bar{\psi}$. Eq. (41) is still qualitatively true, as will be justified below. With these estimates we obtain

$$100 \xi_\beta / N_{\text{av}} L \ll \tilde{\tau}_\beta \ll (L / N \xi_\beta)^3 , \quad (55)$$

$$800 L^2 / N_{\text{av}} \tilde{R} \xi_\beta^2 \mathbf{L}^2 \ll \tilde{\tau}_\beta \ll L^4 / N \tilde{R} \xi_\beta^4 \mathbf{L}^2 . \quad (56)$$

There are two contributions to $\Delta_{\text{mac}} \tilde{\psi}_{\beta k}$: an “internal” contribution $-\tilde{\tau}_\beta (\alpha' + |\tilde{\psi}_{\beta k}|^2) \tilde{\psi}_{\beta k}$, and an “external” contribution due to the interaction with the neighboring elements $k \pm 1$. We are interested in using values of $\tilde{\tau}_\beta$ that are not too small. We found in Sec. III C how

to deal with the external contribution. If only the internal contribution is considered, the evolution equation can be integrated and gives $\tilde{\psi}_{\beta k}(t+\tau) = (\alpha'/[(\alpha' + |\tilde{\psi}_{\beta k}(t)|^2) \exp(2\alpha'\tilde{\tau}_\beta) - |\tilde{\psi}_{\beta k}(t)|^2])^{1/2} \tilde{\psi}_{\beta k}(t)$. Substituting this expression by a computationally less expensive Padé approximant we obtain the algorithm

$$\tilde{\psi}_{\beta k} \leftarrow \frac{2 + (|\tilde{\psi}_{\beta k}|^2 - \alpha')\tilde{\tau}_\beta}{2 + (3|\tilde{\psi}_{\beta k}|^2 + \alpha')\tilde{\tau}_\beta} \tilde{\psi}_{\beta k} \quad (57)$$

that takes into account the internal contribution.

2. Results

Figure 11 shows the average value of $|\psi_{\beta k}|^2$, obtained using Eqs. (53)-(54) and Eq. (57) for a wire of uniform cross section and in a region that includes the critical temperature, as $\tilde{\alpha}$ and \tilde{R} were varied. $|\psi_{\beta k}|^2$ was averaged over N_{av} iteration steps and also over k in the range $1 + N_{\text{cont}} \leq k \leq N - N_{\text{cont}}$. In several cases $\tilde{\alpha}$ was swept downwards and then upwards, in order to check for hysteresis; for the parameters we studied, no evidence for hysteresis was found. As could be expected from Eq. (53), the values of $\langle |\psi_\beta|^2 \rangle$ are a universal function of α' . We also evaluated $\langle |\psi_\beta|^2 \rangle$ for different values of ξ_β/L and L (not shown in Fig. 11), and the results lie on the same curve.

In the considered range, $\langle |\psi_\beta|^2 \rangle$ can be fitted by the empiric expression

$$\langle |\psi_\beta|^2 \rangle = -1.44(\alpha'/2 - \log_e(1 + e^{\alpha'/2})) - 0.70(\alpha' - \log_e(1 + e^{\alpha'})) - 1.93/(1 + e^{\alpha'}) . \quad (58)$$

For the purpose of establishing condition (55) we evaluated $\langle I_{\text{SC}}^2 \rangle$ for zero total current and various values of α' , ξ_β/L , L and \tilde{R} . Some of the results are shown in Fig. 11, and are fitted by $\langle I_{\text{SC}}^2 \rangle^{1/2} = 2.61(\xi_\beta/L)^{1/2} \langle |\psi_\beta|^2 \rangle^{0.58} ek_B T/\hbar$. As a test for linear response, we evaluated $\langle |\psi_\beta|^2 \rangle$ in several cases for zero current and for $I = 0.1ek_B T/\hbar$; the current caused a decrease of $\langle |\psi_\beta|^2 \rangle$ of the order of 0.2%.

Figure 12 shows the superconducting contribution to the electric conductivity for several values of \tilde{R} , L and ξ_β , with α' in the range $-2 \leq \alpha' \leq 2$. The results were fitted by a modification of Eq. (49). Writing $K' = \tilde{R}\xi_\beta^3 L^2/L^3$, we defined the quantity

$$\sigma_{\beta\text{AL}} = (K'\sigma/8)(\alpha' + \langle |\psi_\beta|^2 \rangle + 0.3488 \tanh(0.734 \langle |\psi_\beta|^2 \rangle^{1.5}))^{-3/2} , \quad (59)$$

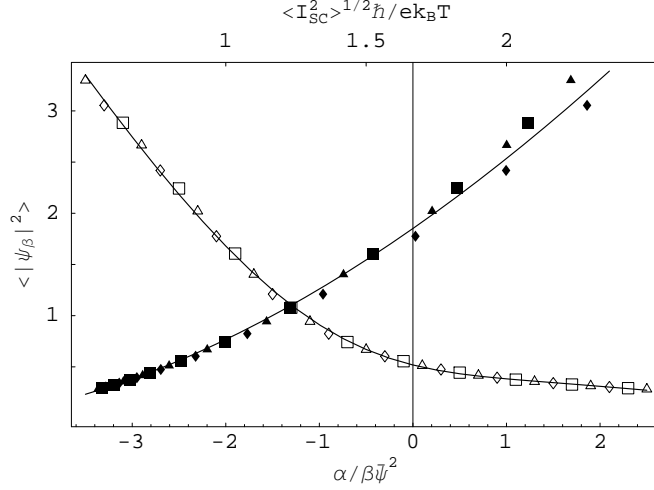


FIG. 11: Average amount of superconducting pairs as a function of α , close to the critical temperature. Empty symbols stand for $\langle |\psi_\beta|^2 \rangle(\alpha')$ (lower abscissa) and are fitted by Eq. (58); filled symbols stand for $\langle |\psi_\beta|^2 \rangle(\langle I_{SC}^2 \rangle)$ (upper abscissa) and are fitted by $\langle I_{SC}^2 \rangle^{1/2} = 2.61(\xi_\beta/L)^{1/2} \langle |\psi_\beta|^2 \rangle^{0.58} e k_B T / \hbar$. $N = 21$, $N_{\text{cont}} = 2$, $N_{\text{av}} = 4 \times 10^7$, $N_{\text{relax}} = 1.2 \times 10^7$, $\xi_\beta = 0.2L$, $L = 10$, $\tilde{\tau}_\beta = 5 \times 10^{-4}$. $\triangle \tilde{R} = 0.1$; $\square \tilde{R} = 3$; $\diamond \tilde{R} = 100$.

which is a generalization of σ_{AL} and reduces to it in the limit $\psi_\beta \rightarrow 0$. $\langle |\psi_\beta|^2 \rangle$ was evaluated using Eq. (58). Finally, the fit used for σ' was

$$\sigma' / \sigma = ((\sigma_{\beta\text{AL}} / \sigma)^{-4/5} + 1.205(\sigma_{\beta\text{AL}} / \sigma)^{-0.23})^{-5/4}. \quad (60)$$

3. Voltage distribution

In the previous sections we have evaluated the time average of the voltage. In this section we investigate how the voltage fluctuates over time steps. We define $L' = (1 - 2N_{\text{cont}}/N)L$, the length of the wire excluding the contact regions, and the dimensionless normalized voltage $\tilde{V} = \gamma e V / \beta \bar{\psi}^2$. For a single step, the normalized voltage drop over L' is $\tilde{V} = -\sum_{k=1+N_{\text{cont}}}^{N-N_{\text{cont}}} \Delta \tilde{A}_k / 2\tilde{\tau}_\beta$.

Figure 13 is a set of histograms for the values of \tilde{V} obtained in every step, for several values of α' . \tilde{V} has contributions from $\Delta_{\text{mac}} \tilde{A}_k$ in Eq. (54) and also from the fluctuations of \tilde{A}_k . Since the fluctuations of \tilde{A}_k are known to be gaussian, the results we present take into account the contribution from $\Delta_{\text{mac}} \tilde{A}_k$ only. These histograms have been fitted by gaussian distributions.

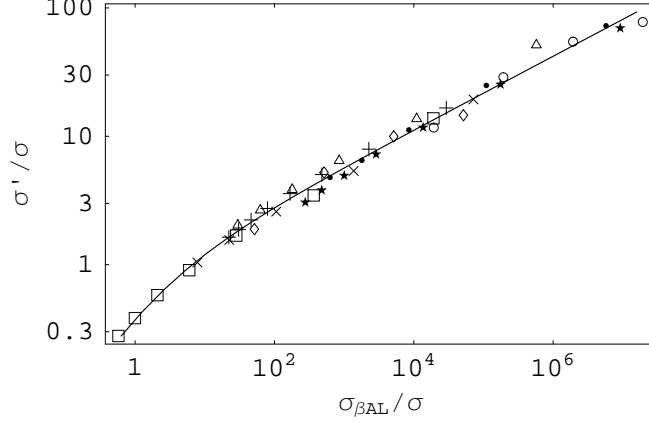


FIG. 12: Superconducting contribution to the electric conductivity in a region where the order parameter is not small. The symbols were evaluated using Eq. (46). The line was evaluated using Eq. (60). Unless stated otherwise, $N = 21$, $N_{\text{cont}} = N/7$, $N_{\text{av}} = 2 \times 10^8$, $N_{\text{relax}} = 6 \times 10^7$, $\xi_\beta = 0.2L$ and $L = 100$. $\tilde{\tau}_\beta = 10^{-4}$ for $\tilde{R} < 30$ and $L < 400$; otherwise, $\tilde{\tau}_\beta = 10^{-5}$. $I = 0.1ek_BT/\hbar$, except for the two leftmost squares, for which $I = 0.2ek_BT/\hbar$. $\square \tilde{R} = 0.1$; $\triangle \tilde{R} = 3$; $\bullet \tilde{R} = 30$; $+ \tilde{R} = 2$, $L = 200$; $\star \tilde{R} = 3$, $L = 400$; $\times \tilde{R} = 3$, $\xi_\beta = 0.1L$, $N = 42$; $\diamond \alpha' = -1.146$ ($\langle |\psi_\beta|^2 \rangle = 1$); $\circ \alpha' = -2$.

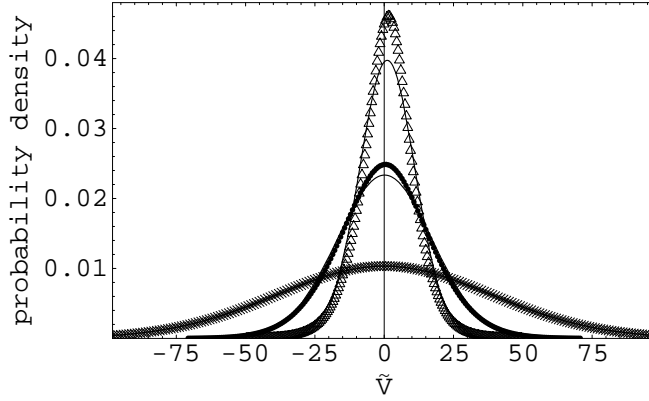


FIG. 13: Distribution of the voltage drop along the wire, evaluated for single steps. $L' = 2.5\xi_\beta$, $I = 0.3ek_BT/\hbar$, $L = 30$, $\tilde{R} = 1$, $N = 15$, $N_{\text{cont}} = 3$, $\tilde{\tau}_\beta = 5 \times 10^{-4}$, $N_{\text{av}} = 2 \times 10^8$, $N_{\text{relax}} = 6 \times 10^7$. The solid line is the gaussian distribution $(2\pi(\langle \tilde{V}^2 \rangle - \langle \tilde{V} \rangle^2))^{-1/2} \exp[-(\tilde{V} - \langle \tilde{V} \rangle)^2 / (2(\langle \tilde{V}^2 \rangle - \langle \tilde{V} \rangle^2))]$. $\triangle \alpha' = -0.5$; $\bullet \alpha' = -2$; $\times \alpha' = -8$.

From Fig. 13 we might conclude that the voltage distribution is approximately gaussian, but such a conclusion would be misleading, since the voltage drops for steps that are close in time are correlated. A more informative distribution is that of the “consecutive phase

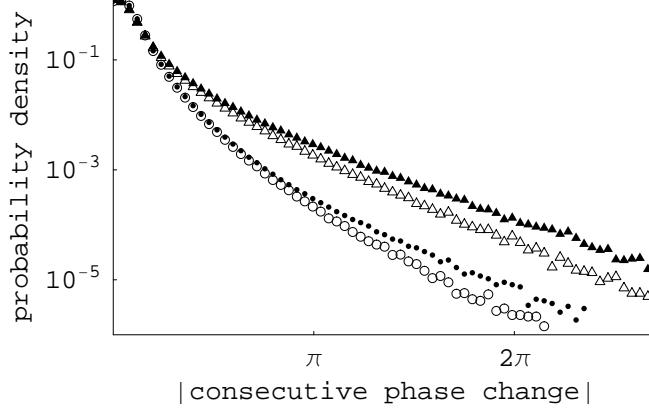


FIG. 14: Distribution of the absolute values of “consecutive phase changes.” Empty symbols are for positive changes of the phase and filled symbols for negative changes. Unless stated otherwise, the parameters are the same as in Fig. 13. $\triangle \alpha' = -0.5$; $\circ \alpha' = -2$, $N_{\text{av}} = 8 \times 10^8$.

change,” which we define as follows. For every step we check the sign of the macroscopic contribution to the phase increment, $\sum_{k=1+N_{\text{cont}}}^{N-N_{\text{cont}}} \Delta \tilde{A}_k$, and add all the consecutive increments until the sign is reversed. Note that in order to decide when to stop adding increments and start evaluating the next phase change we monitored only the macroscopic contribution to $\sum \Delta \tilde{A}_k$, but in order to evaluate these increments we took into account the microscopic fluctuations as well. The results are shown in Fig. 14. Although the sizes of typical voltage drops in a single step increase when α' becomes more negative, we see that the probability of large phase excursions is greater for $\alpha' = -0.5$ than for $\alpha' = -2$. We also see that the probability of large negative phase changes is greater than that of large positive phase changes, and this explains the average voltage drop.

According to the Langer–Ambegaokar–McCumber–Halperin (LAMH) scenario [21], the voltage drop is due to “phase slips,” in which the phase decreases by 2π . Accordingly, we expected to find a relatively large probability density near 2π in Fig. 14, but we did not obtain support for this view.

4. *Scaling with length*

In the previous sections we have tacitly assumed that the voltage drop along a uniform wire is proportional to its length. We have taken advantage of this assumption and considered short wires, that do not require large computational resources. In this section we check

TABLE II: Voltage drop and its variance, per unit length of the wire. L' is the length (excluding the contact regions) over which V is evaluated. The parameters used are $\tilde{R}/L = 0.033$, $I = 0.3ek_BT/\hbar$, $\xi_\beta = 7.2\hbar/\sqrt{2mk_BT}$, $N_{\text{cont}} = 3$, $N = 6 + 3.6L'/\xi_\beta$, $\tilde{\tau}_\beta = 5 \times 10^{-4}$, $N_{\text{av}} = 2 \times 10^8$, $N_{\text{relax}} = 6 \times 10^7$.

	$10^3(\gamma e/k_BT)\xi_\beta\langle V\rangle/L'$			$10^2(\gamma e/k_BT)^2\xi_\beta(\langle V^2\rangle - \langle V\rangle^2)/L'$		
α'	$L' = 2.5\xi_\beta$	$L' = 10\xi_\beta$	$L' = 30\xi_\beta$	$L' = 2.5\xi_\beta$	$L' = 10\xi_\beta$	$L' = 30\xi_\beta$
-0.5	8.48	8.87	8.97	1.52	1.58	1.75
-1	5.89	6.31	6.42	2.11	2.15	2.23
-2	1.26	1.31	1.30	4.35	4.48	4.52

this assumption. We have evaluated the voltage and its variance for several values of α' and several lengths, while intrinsic quantities such as \tilde{R}/L are kept at a fixed value. The results are summarized in Table II. The average of the voltage per unit length, and its variance per unit length, which should in principle be independent of L' , seem to increase slightly with L' ; in the case of $\langle V\rangle/L'$, this trend seems to saturate within the considered range. The deviations from the proportionality $\langle V\rangle \propto L'$ are most likely due to the finite sizes of the elements of the computational grid and of the contact regions.

5. Comparison with experiments

It is usually accepted that different models are required for the description of the electric conductivity in several temperature ranges in the vicinity of the critical temperature. Above the critical temperature, conductivity is believed to be dominated by the exchange of “cooperons” between normal electrons [22]. Very near the critical temperature, a promising method is the Hartree-Fock approximation to TDGL [14]. Below the critical temperature, but not too near it, the LAMH model gives good fits [21]. For still lower temperatures there is a “foot” which some authors attribute to the contacts [23] and others to macroscopic quantum tunneling [17]. Moreover, the parameters we have studied in section IV C 2 differ by several orders of magnitude from those of the available experimental data. In spite of this situation, it is instructive to check how well our naive formalism can fit the experimental data.

We analyzed samples of aluminum [16], indium [17] and tin [18], in a temperature range

where $10^{-2}\sigma \lesssim \sigma' \lesssim 10^{1.5}\sigma$. We chose the samples so that they could be considered as one-dimensional, sufficient data in the analyzed range were available and all the required properties of the sample (e.g. length) were reported. We denote by T'_c the temperature that the experimenters considered to be the critical temperature. The data for aluminum are above T'_c and the others below T'_c . The normal resistance of the tin sample was smaller by more than three orders of magnitude than those of the other samples; this was due both to its larger cross section and its longer mean free path. The current passed through the tin sample was slightly above the linear range.

The properties of a sample were estimated as follows. The length was measured by means of a microscope; the cross section was either estimated from microscopic observation or from the critical current. Assuming the geometry is known, the mean free path can be obtained from the normal conductivity [24]. The BCS coherence length and the London penetration depth are assumed to be the same as in bulk material, in spite of the fact that the critical temperature is significantly different than that in bulk. $\xi(0)$ and κ can be obtained from these values and the mean free path [23], and ξ_β from Eq. (52). T'_c is either assumed equal to the critical temperature of a reference sample with large cross section, or is taken from a fit to some model. For γ we take the value $\pi\hbar^2/16k_B T'_c m \xi(0)^2$.

We denote by $\Delta T = T'_c - T_c$ the difference between the the critical temperature estimated by the experimenters and that required by our model. We fitted the experimental data using our phenomenological Eqs. (58)–(60), with $\xi(0)$, ξ_β and ΔT as free parameters. The results are shown in Figs. 15–16; there is semiquantitative agreement, but the fitting functions are too concave.

The values of the fitting parameters $\xi(0)$, ξ_β and ΔT are displayed in Table III. They cannot be taken too seriously, because it is possible to increase or decrease simultaneously the three parameters in a wide range without bringing about a clear difference in the goodness of the fit; moreover, the values of these parameters depend on the selected range. In all cases, T_c is reasonably close to T'_c ; for comparison, for the In microwires T'_c differs by $\sim 800\text{mK}$ from the critical temperature in bulk.

$\xi(0)$ and ξ_β enter our equations in two ways. One of them is through α' , and in this case only their ratio $\xi_\beta/\xi(0)$ is of influence. In all cases, the experimental and the fitted ratio differ by less than half an order of magnitude, a factor that can be attributed to the coarse estimates, both in the experiment and in the fit. $\xi(0)$ or ξ_β themselves enter through K' ,

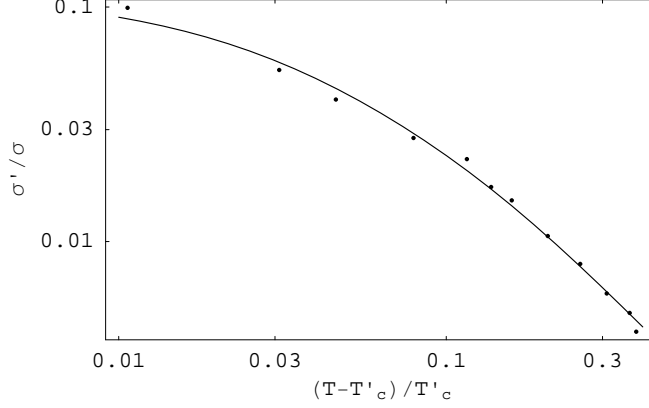


FIG. 15: Paraconductivity of an aluminum microwire as a function of the temperature above T'_c . The dots are experimental data and the curve is a fit using Eqs. (58)–(60).

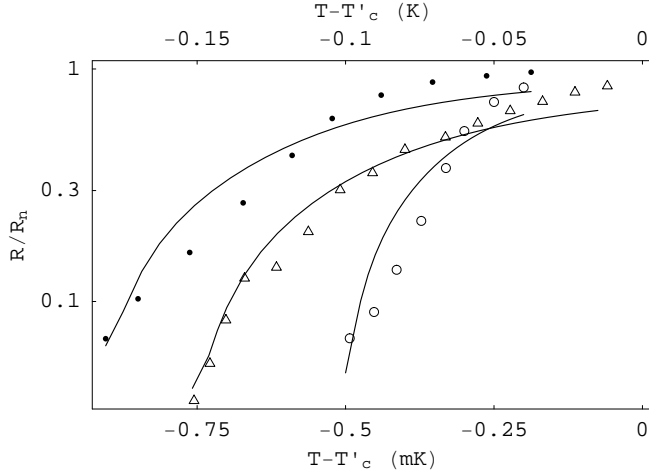


FIG. 16: Resistances of indium microwires (upper scale) and a tin whisker (lower scale) as functions of temperature. R is the resistance of the sample and R_n is its resistance in the normal state. \triangle Sn, $w_0 \sim 2 \times 10^{-9} \text{cm}^2$; \bullet In, $w_0 \sim 1.7 \times 10^{-11} \text{cm}^2$; \circ In, $w_0 \sim 5.2 \times 10^{-11} \text{cm}^2$.

which in turn depends on the assumption $\gamma = \pi \hbar^2 / 16 k_B T'_c m \xi(0)^2$; in this case it seems that $\xi(0)^{\text{fit}}$ and ξ_β^{fit} are too big. This might indicate that the theory for γ is inappropriate and a more elaborate theory might be required [25].

D. A constriction

We deal now with the case for which the present formalism has been designed, namely, a wire with nonuniform cross section. Denoting the arclength by s , we consider a wire such

TABLE III: Parameters used in Eqs. (58) and (59)

for the theoretical lines in Figs. 15–16. “exp” stands for the values estimated in the experiments and “fit” corresponds to the present fit. ΔT is the difference between the critical temperatures estimated in the experiments and those required here. The lengths $\xi(0)$ and ξ_β are expressed in μm . $\xi(0)^{\text{exp}}$ is not the same for the thin and the wide In wires, because they have different mean

free paths.					
	ΔT (mK)	$\xi(0)^{\text{exp}}$	$\xi(0)^{\text{fit}}$	ξ_β^{exp}	ξ_β^{fit}
Al	22	0.15	1.1	3.1	5.8
In (thin)	83	0.042	0.33	1.0	3
In (wide)	55	0.071	0.42	3.1	5.6
Sn	0.355	0.22	14	20	1870

that its cross section is uniform in segments of length $N_{\text{cont}}L/N$ at each extreme, assumes the value $w_{\text{ctr}} \neq w_0$ at the position $s = s_{\text{ctr}}$, $N_{\text{cont}}L/N < s_{\text{ctr}} < L - N_{\text{cont}}L/N$, and is linear in s for $N_{\text{cont}}L/N \leq s \leq s_{\text{ctr}}$ and $s_{\text{ctr}} \leq s \leq L - N_{\text{cont}}L/N$. We denote by w_0 the average cross section in the examined region $N_{\text{cont}}L/N \leq s \leq L - N_{\text{cont}}L/N$, i.e. the cross section in the contact regions has to be $2w_0 - w_{\text{ctr}}$. If $w_{\text{ctr}} < w_0$ there is a constriction, and in the opposite case there is a widening. We still use the notations $\tilde{R} = 4e^2\gamma L/\hbar\sigma w_0$, $\xi_\beta = (\hbar^4 w_0/4\beta m^2 k_B T)^{1/3}$. In the discretized version we identify w_i with the cross section at $s = (i - 1/2)L/N$.

1. Conductivity

With these notations, Eq. (46) has to be replaced with

$$\frac{\sigma'}{\sigma} = \frac{(N - 2N_{\text{cont}})\tilde{R}\hbar I w_0/e}{8N\gamma e\langle V\rangle(w_0 - w_{\text{ctr}})} \log \frac{2w_0 - w_{\text{ctr}}}{w_{\text{ctr}}} - 1, \quad (61)$$

where V is the potential drop excluding the initial and the final N_{cont} elements.

Figure 17 compares the conductivities of a uniform and two nonuniform wires, as functions of the temperature. As the temperature decreases, the conductivities of the nonuniform wires increase at lower rates. An intuitive reason could be that in the thinner parts of the wire fluctuations are more effective in breaking superconductivity. Several evaluations of σ'

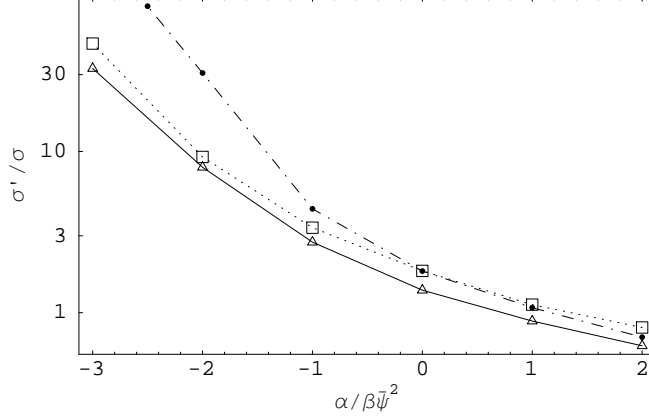


FIG. 17: Contribution of superconductivity to the conductivities of a uniform and two nonuniform wires, as functions of the temperature. Unless stated otherwise, $L = 10$, $\tilde{R} = 100$, $s_{\text{ctr}} = 0.5L$, $\xi_\beta = 0.2L$, $I = 0.1ek_BT/\hbar$, $N = 21$, $N_{\text{cont}} = 3$, $\tilde{\tau}_\beta = 5 \times 10^{-4}$, $N_{\text{av}} = 2 \times 10^8$, $N_{\text{relax}} = 6 \times 10^7$. For visibility, the symbols have been joined by straight segments. ● uniform wire; △ $w_{\text{ctr}} = 0.2w_0$; □ $w_{\text{ctr}} = 1.8w_0$.

were repeated for different currents and we verified that our results correspond to the linear regime.

2. Charge accumulation

As a last test for statistical mechanics, we disconnect the current source and connect a capacitor C between the points $s = 0$ and $s = s_C$. This capacitor will be charged with a charge Q that fluctuates in time. The region $0 \leq s \leq s_C$ will be forced to sustain a potential drop Q/C and the current I_1 in this region will be obtained as a Lagrange multiplier, as in Sec. III E. The current in the region $s_C \leq s \leq L$ has to vanish. During each step, the charge in the capacitor increases by the amount $I_1\tau$.

From the point of view of the capacitor, the wire is just a heat reservoir. Therefore, writing $\tilde{Q} = Q/\sqrt{k_B T C}$, the probability density for the charge will be proportional to $\exp(-\tilde{Q}^2/2)$. From here, we expect $\langle |\tilde{Q}|^n \rangle = 2^{n/2} \Gamma((n+1)/2) / \sqrt{\pi}$. Table IV compares this prediction with the results obtained with our formalism.

TABLE IV: Average value of $|\tilde{Q}|^n$ according to statistical mechanics and to the method developed here. $s_{\text{ctr}} = 0.36L$, $s_C = 0.48L$, $C = 0.01\gamma^2 e^2/k_B T$; the other relevant parameters are as in Fig. 17.

n	1	2	3	4
$2^{n/2}\Gamma((n+1)/2)/\sqrt{\pi}$	0.80	1	1.60	3
our simulation	0.81	1.02	1.65	3.14

V. SUMMARY

We have developed a formalism that takes into account the influence of thermal fluctuations in a one-dimensional superconductor described by the TDGL model. Our method relies on the fluctuation-dissipation theorem and, accordingly, complies with statistical mechanics. We have explicitly addressed the case in which the evolution equations are solved by means of finite differences and pointed out the relationship between the size of the fluctuations and the volume of the elements into which the sample is divided. To my knowledge, this relationship has not been previously addressed in the literature.

Using a gauged order parameter ($\tilde{\psi}$) rather than the raw order parameter (ψ), we obtain a formalism in which the electromagnetic potential is not needed in the macroscopic evolution. Special care is required in the use of this transformation; although the thermodynamic potential is more naturally expressed in terms of $\tilde{\psi}$, the variable that permits direct application of the fluctuation-dissipation theorem is ψ .

As an application we have evaluated the contribution of incipient superconductivity to the electrical conductivity. Significantly above the critical temperature, we recover the Aslamazov-Larkin result. We have focused on the regime immediately below the critical temperature. We compared our results with those of old experiments in this regime, and the agreement is poor. On the other hand, no available theory reproduces the experimental data in this regime, although the Hartree approximation has been successful in situations in which fluctuations may be regarded as effectively one-dimensional [26].

Our formalism can be easily generalized to higher dimensionality, multiply connected topologies where non-integer fluxes are enclosed, time-dependent applied voltages or currents, or different evolution equations that can be cast in the form of dissipative equations.

Acknowledgments

This work has been supported by the Israel Science Foundation under grant 4/03-11.7.

- [1] P. Langevin, C. R. Acad. Sci. (Paris) **146**, 530 (1908). See also D. S. Lemons and A. Gythiel, Am. J. Phys. **65**, 1079 (1997).
- [2] L. P. Gor'kov and G. M. Eliashberg, Zh. Eksp. Teor. Fiz. **54**, 612 (1968) [Soviet Phys. JETP **27**, 328 (1968)]; A. Schmid, Phys. Kondens. Mater. **5**, 302 (1966); M. Cyrot, Rep. Prog. Phys. **36**, 103 (1973).
- [3] A. Schmid, Phys. Rev. **80**, 527 (1969).
- [4] R. Kato, Y. Enomoto and S. Maekawa, Phys. Rev. B **47**, 8016 (1993).
- [5] C. Bolech, G. C. Buscaglia and A. López, Phys. Rev. B **52**, R15719 (1995).
- [6] M. Ghinovker, B. Ya. Shapiro and I. Shapiro, Europhys. Lett. **53**, 240 (2001).
- [7] M. Karttunen, K. R. Elder, M. B. Tarlie, and M. Grant, Phys. Rev. E, **66**, 026115 (2002).
- [8] J. Berger and J. Rubinstein, Phys. Rev. Lett. **75**, 320 (1995); Phys. Rev. B **59**, 8896 (1999); J. Berger, in *Connectivity and Superconductivity*, edited by J. Berger and J. Rubinstein (Springer, Berlin, 2000).
- [9] S.V. Dubonos, V.I. Kuznetsov, I.N. Zhilyaev, A.V. Nikulov, and A.A. Firsov, Pis'ma Zh. Eksp. Teor. Fiz. **77**, 439 (2003) [JETP Lett. **77**, 371 (2003)].
- [10] G. Richardson and J. Rubinstein, Proc. R. Soc. Lond. A **455**, 2549 (1999).
- [11] A. T. Dorsey and M. P. A. Fisher, Phys. Rev. Lett. **68**, 694 (1992).
- [12] M. Machida and M. Itakura, Physica C **392-396**, 331 (2003).
- [13] F. Reif, *Fundamentals of Statistical and Thermal Physics* (McGraw-Hill, Kogakusha, 1965); R. Kubo, M. Toda, and N. Hashitsume, *Statistical Physics II* (Springer, Berlin, 1995).
- [14] J. R. Tucker and B. I. Halperin, Phys. Rev. B **3**, 3768 (1971).
- [15] L. G. Aslamazov and A. I. Larkin, Fiz. Tver. Tela **10**, 1104 (1968) [Soviet Physics - Solid State **10**, 875 (1968)].
- [16] A. F. Mayadas and R. B. Laibowitz, Phys. Rev. Lett. **28**, 156 (1972).
- [17] N. Giordano, Phys. Rev. Lett. **61**, 2137 (1988); N. Giordano, Phys. Rev. B **41**, 6350 (1990); N. Giordano, Phys. Rev. B **43**, 160 (1991).

- [18] E. Lukens, R. J. Warburton, and W. W. Webb, Phys. Rev. Lett. **25**, 1180 (1970); R. S. Newbower, M. R. Beasley, and M. Tinkham, Phys. Rev. B **5**, 864 (1972).
- [19] J. W. Cook, M. J. Skove, E. P. Stillwell, and R. S. Thompson, Phys. Lett. **32A**, 445 (1970).
- [20] P. Santhanam, C. C. Chi, S. J. Wind, M. J. Brady, and J. J. Bucchignano, Phys. Rev. Lett. **66**, 2254 (1991).
- [21] J. S. Langer and V. Ambegaokar, Phys. Rev. **164**, 498 (1967); D. E. McCumber and B. I. Halperin, Phys. Rev. B **1**, 1054 (1970).
- [22] K. Maki, Prog. Theor. Phys. (Kyoto) **40**, 193 (1968); R. S. Thompson, Phys. Rev. B **1**, 327 (1970); B. Patton, Phys. Rev. Lett. **27**, 1273 (1971); A. Larkin and A. Varlamov, *Theory of Fluctuations in Superconductors* (Oxford University, 2005).
- [23] M. Tinkham, *Introduction to Superconductivity* (Dover, 1996).
- [24] I. Holwech and J. Jeppesen, Phil. Mag. **15**, 217 (1967); K. R. Lyall and J. F. Cochran, Phys. Rev. **139**, 517 (1967).
- [25] L. Kramer and R. J. Watts-Tobin, Phys. Rev. Lett. **40**, 1041 (1978).
- [26] V.A. Marchenko and A.V. Nikulov, Physica C **210**, 466 (1993); A. V. Nikulov, D. Yu. Remisov and V. A. Oboznov, Phys. Rev. Lett. **75**, 2586 (1995).